ISBN: 978-3-95450-247-9 ISSN: 2673-5490 doi: 10.18429/JACoW-IPAC2024-MOPR93

# NEUTRON PRODUCTION USING COMPACT LINEAR ELECTRON ACCELERATORS

J. Olivares Herrador * [1,2], L. Wroe [1], A. Latina [1], W. Wuensch [1], R. Corsini [1], S. Stapnes [1], N. Fuster-Martinez [2], B. Gimeno [2], D. Esperante [2,3]
[1] CERN, Geneva, Switzerland
[2] Instituto de Física Corpuscular (IFIC); CSIC-University of Valencia, Paterna, Spain
[3] Department of Electronic Engineering—ETSE, University of Valencia, Burjassot, Spain



*Abstract*

There is an increasing demand for neutron-based analysis beamlines for a wide range of scientific and industrial applications. However, many reactor-based neutron sources are scheduled to be shut down in the near future. Consequently, compact accelerator-based neutron sources are a competitive alternative that could meet the imminent need for medium-flux fission or spallation sources. In this report, we explore the performance of compact electron accelerators as neutron drivers and propose a preliminary target design for a high-gradient electron-linac-based neutron source.

## INTRODUCTION

Since the late 1950s, research nuclear reactors built in numerous laboratories and universities have been used as neutron sources. These particles offer a wide range of applications in diverse areas, including material science, nuclear medicine, spectroscopy and imaging [1]. An overview of these applications and the required neutron energy and intensities is shown in Fig. 1.

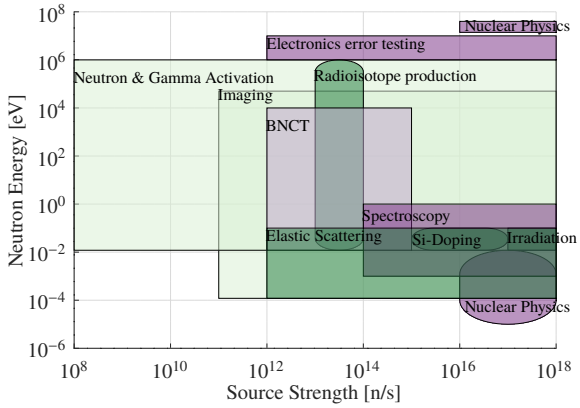


Figure 1: Neutron applications chart. Data extracted from [1] and [2].

However, many of these reactors plan to shut down soon primarily due to the fear of reactor-related incidents [3]. There is nevertheless the continued need to supply high-intensity neutron beams, and accelerator-driven neutron sources have been constructed in recent years to support and develop neutron activities.

* javier.olivares.herrador@cern.ch

Two different types of accelerator-based neutron sources are found: spallation sources and compact accelerator-based neutron sources (CANS). In the spallation process, protons are accelerated to high energies to collide with a high atomic number material such as lead, tungsten or mercury. This technique produces high fluxes of neutrons at the cost of the expensive and high-power consuming installations required to accelerate protons to hundreds of MeVs [4].

CANS on the other hand are based on both proton and electron linacs. These sources offer a more compact and affordable alternative which becomes highly competitive to existing medium flux fission or spallation based sources [5]. A summary of the most representative facilities of the state-of-art can be found in Fig. 2.

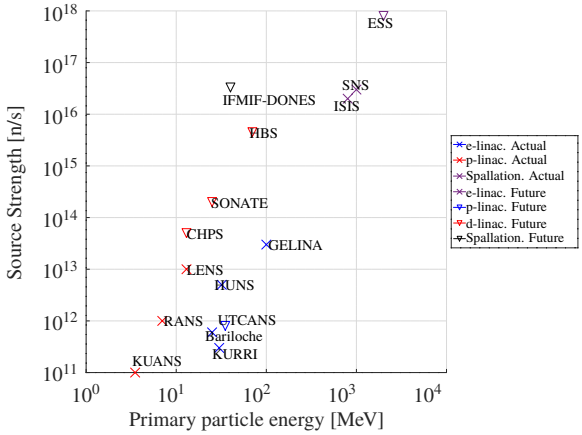


Figure 2: Source strength vs primary particle energy. Data from [6–9].

In this document, the performance of electron linacs as CANS drivers is explored. To do so, a cylindrical tungsten target is optimized for maximum neutron yield and the direction and energy dependency of its emission is analyzed. Then, two specific high gradient electron linacs are proposed as drivers for this optimized target, and their source strengths in terms of primary energy and beam power is compared with the state-of-art facilities and designs.

## TUNGSTEN TARGET OPTIMIZATION FOR NEUTRON PRODUCTION

To produce neutrons with electron accelerators in the MeV range, the dominant process consists of two steps: first,

ISBN: 978-3-95450-247-9 ISSN: 2673-5490 doi: 10.18429/JACoW-IPAC2024-MOPR93

gamma photons are created via electron bremsstrahlung against a high Z material. These photons then excite the nucleus of a second target (in this case, the same tungsten target), from which neutrons are emitted, among other particles. A detailed description on the efficiency and spectrum of each process can be found in [4].

Electron, photon and neutron transport and creation in these scenarios have been simulated with `g4beamlines` [10], a software which uses Monte Carlo random number sampling to study radiation-matter interaction. By making use of the library QGSP_BIC_HP, specific photonuclear cross sections are imported from ENDF-VIII.0, JEFF-3.3 [11], thus enabling the simulation of neutronic processes at energies below 20 MeV.

In order to examine neutron production, the following figures of merit are considered.

$$\begin{aligned} &\text{Average yield} && Y_{n,av} = \frac{N_n}{N_q} && \left[\tfrac{\text{n}}{\text{e}}\right] \\ &\theta\text{-distribution} && f_\theta = \frac{1}{2\pi}\int_0^{2\pi} \mathrm{d}\varphi \frac{\mathrm{d}Y_n}{\mathrm{d}\Omega} && \left[\tfrac{\text{n}}{\text{e}\cdot\text{rad}}\right] \\ &E_n\text{-spectrum} && f_{\theta,E_n} = \frac{\mathrm{d}f_\theta}{\mathrm{d}E_n} && \left[\tfrac{\text{n}}{\text{e}\cdot\text{rad}\cdot\text{MeV}}\right]. \end{aligned}$$

Here, $N_q$ stands for the total number of primary particles $q$ arriving at the target in an RF cycle, $N_n$ is the total number of neutrons emitted in all directions and $\Omega(\theta_d, \varphi) = \int_0^\varphi \mathrm{d}\varphi \int_0^\theta \mathrm{d}\theta_d \sin\theta_d$ is the solid angle of detection with $0 \leq \varphi < 2\pi$ and $0 \leq \theta_d < \pi$.

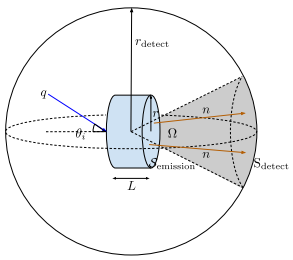


Figure 3: Spherical geometry for neutron production and detection when a charge $q$ hits a tungsten target (in blue).

To investigate the optimal shape of a single tungsten target for neutron production by electrons, a cylindrical tungsten target of radius $r = 50$ mm and length $L$ has been studied, as illustrated in Fig. 3. The results of a scan in $L$ for different electron energies ($\langle E_e \rangle$) was performed, and the results are shown in Figs. 4a and 4b.

These results show that backward neutron production ($\pi/2 \leq \theta_d < \pi$ rad) is greater than forward neutron production ($0 \leq \theta_d < \pi$ rad). A good compromise between forward and backward production is found for $L = 80$ mm, which is hereafter assumed in this work.

## *Directional Neutron Production*

The cylindrical symmetry of the problem results in an isotropic average-yield. Fig. 5a shows that the total neutron

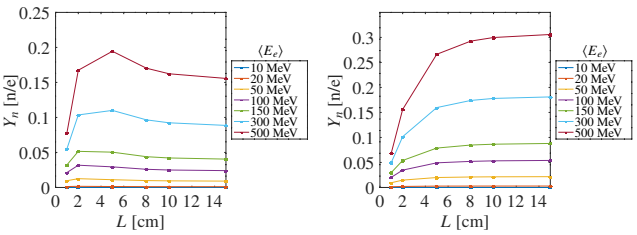


(a) Forward neutron yield. (b) Backward neutron yield.

Figure 4: Neutron yield for a single tungsten target as a function of the target length.

production remains unaltered when the polar-incident angle $\theta_i$ varies from 0 to 40 degrees for all electron energies. In addition, Fig. 5b shows that the detection is also isotropic for $140 \leq \theta_d \leq 180$ degrees.

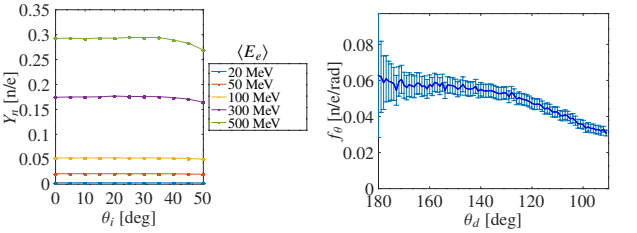


(a) Backward $Y_n$ vs. $\theta_i$. (b) Backward $f_\theta$ for $\theta_i = 0°$ and $\langle E_e \rangle = 500$ MeV

Figure 5: Directional backward neutron emission.

## *Neutron Energy*

For incident electron energies of $\langle E_e \rangle = 20$ - 500 MeV, the characteristics of the energy spectrum of the emitted neutrons are summarized in Table 1. It can be seen that the mean energy of the emitted neutrons ranges from 0.8 to 1.1 MeV and that the energy spread scales with electron energy.

Table 1: Backward $f_\theta$, $\langle E_n \rangle$ and $\sigma_{E_n}$ for the Neutron Spectrum Emerging at $\theta_d = 155°$ for Different Electron Energies

| $E_e$ [MeV] | $\langle E_n \rangle$ [MeV] | $\sigma_{E_n}$ [MeV] |
|---|---|---|
| 20 | 0.776 | 0.625 |
| 50 | 0.859 | 0.741 |
| 100 | 0.986 | 0.973 |
| 300 | 1.08 | 1.15 |
| 500 | 1.08 | 1.17 |

Figure 6a shows the energy spectrum for each detecting direction at $\langle E_e \rangle = 500$ MeV and Fig. 6b shows the energy spectrum for $\theta_d = 155°$, where a Maxwellian distribution of the emitted neutrons can be observed with a peak around the mentioned value of 0.8 MeV. Some high energy neutrons are detected as well at approximately 10 MeV, thus justifying the high $\sigma_{E_n}$ value in Table 1 in addition to the shift of $\langle E_n \rangle$ from the peak value to the one in Table 1.

ISBN: 978-3-95450-247-9 ISSN: 2673-5490 doi: 10.18429/JACoW-IPAC2024-MOPR93



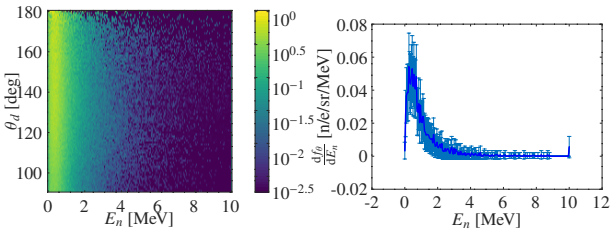


(a) Backward energy spectrum at for $\theta_i = 0°$ and $E_e = 500$ MeV.

(b) Backward energy spectrum for $\theta_i = 0°$ and $E_e = 500$ MeV at $\theta_d = 155°$.

Figure 6: Energy spectrum.

## HIGH-GRADIENT ELECTRON LINAC CANS STRENGTH

The performance of a neutron source can be assessed by studying its source strength, defined as the neutron intensity emitted over a solid angle of $4\pi$ steradians [2]. For the case of an electron linac based CANS, the source strength is related to the neutron yield as:

$$I_n = I_{e,\mathrm{av}} Y_{n,\mathrm{av}}, \tag{1}$$

where $I_{e,\mathrm{av}}$ is the electron beam current provided from the linac driver.

For the optimized target length of $L_{\mathrm{target}} = 80$ mm and incident electron direction of $\theta_i = 0°$, the source strength has been calculated for two electron linacs: CLIC Test-Facility 3 (CTF3) drive beam linac [13] and High-Pulse-Current-Injector (HPCI) [12]. Their details are shown in Tab. 2

Table 2: Specifications of the Considered Electron Linacs [12, 13]

| Magnitude | Units | HPCI-linac | CTF3 d.b. linac |
|---|---|---|---|
| $f$ | GHz | 2.998 | 11.99 |
| $Q_{\mathrm{bunch}}$ | nC | 0.285 | 2.33 |
| $N_{\mathrm{bunches}}$ | | 1000 | 2100 |
| $f_{\mathrm{RF\ cycle}}$ | Hz | 100 | 100 |
| $I_{e,\mathrm{av}}$ | $\mu$A | 28.50 | 489.3 |

Fig. 7 shows the scaling of the source strength of the proposed high gradient electron-linac based CANS with the incident beam energy, ranging from 20 to 500 MeV. These values are represented along with the comparison to existing sources in Fig. 2. It can be seen that the proposed electron linac based CANS can reach neutron intensities up to $\simeq 10^{15}$ n/s.

The CANS source strength depends on the electron intensity as well as its energy as seen in Eq. (1) and Fig. 7. In other words, the source strength is highly dependent on the electron beam power, defined as:

$$P_{\mathrm{beam}}[\mathrm{W}] = I_{e,\mathrm{av}}[\mathrm{A}] E_e[\mathrm{eV}]/\mathrm{e}. \tag{2}$$

Based on Fig. 7 and Eq. 2, the dependency on the neutron strength with the beam power is illustrated in Fig. 8, which shows that both electron and positron CANS exhibit a linear dependency of the source strength with the beam power.

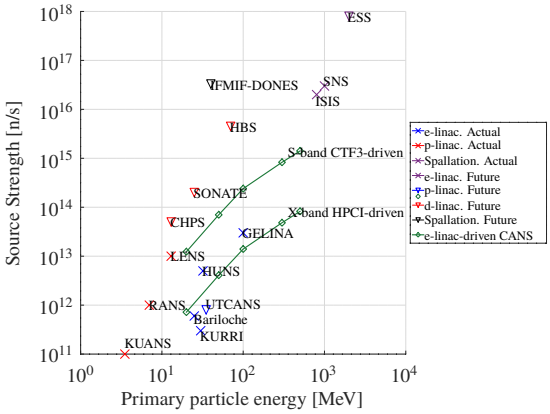


Figure 7: Source strength vs primary energy particle. The uncertainty of the proposed e-linac CANS source strength (in green) is inferior to the marker size.

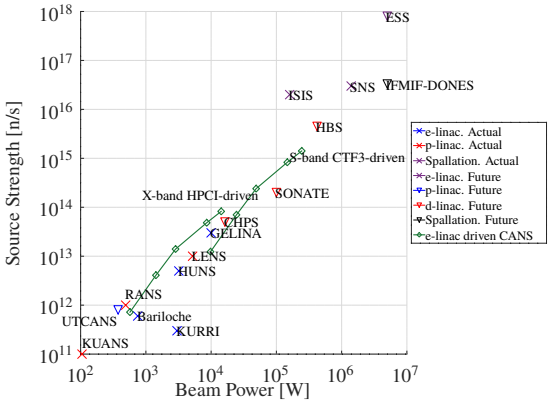


Figure 8: Source strength vs average beam power for the proposed electron linacs and for the state of art. The uncertainty of the proposed e-linac CANS source strength (in green) is inferior to the marker size.

## CONCLUSION

The state of art of neutron production has been reviewed and compared to the performance achievable from an electron-linac-based CANS. This was assessed by optimizing the dimensions of a cylindrical tungsten target and calculating the neutron source strength for two high-gradient electron accelerators operating at different electron energies.

It is shown that such a CANS scheme provides a competitive neutron strength (up to $10^{15}$ n/s) which could serve many neutron applications.Without moderating the neutrons, the current configuration could serve for irradiation studies.

This report provides the basis for future work where a moderator-target assembly could be optimized to fulfill the requirements of an specific applications such as imaging or spectroscopy.

ISBN: 978-3-95450-247-9 ISSN: 2673-5490 doi: 10.18429/JACoW-IPAC2024-MOPR93

## REFERENCES


[1] Y. Kiyanagi, "Neutron applications developing at compact accelerator-driven neutron sources,"AAPPS Bulletin, vol. 31, no. 1, Sep. 2021. doi:10.1007/s43673-021-00022-3

[2] Compact Accelerator Based Neutron Sources, ser. TECDOC Series. Vienna: IN-TERNATIONAL ATOMIC ENERGY AGENCY, 2021, no. 1981. [Online]. Available: https://www.iaea.org/publications/14948/compact-accelerator-based-neutron-sources

[3] J. M. Carpenter, "The development of compact neutron sources,"*Nat. Rev. Phys.*, vol. 1, no. 3, pp. 177–179, Jan. 2019. doi:10.1038/s42254-019-0024-8

[4] H. Feizi and A. H. Ranjbar, "Developing an Accelerator Driven System (ADS) based on electron accelerators and heavy water,"*IEEE Open J. Instrum. Meas.*, vol. 11, no. 02, pp. P02004–P02004, Feb. 2016. doi:10.1088/1748-0221/11/02/p02004

[5] T. Brückel, T. Gutberlet, S. Schmidt, C. Alba-Simionesco, F. Ott, and A. Menelle, "Low energy accelerator-driven neutron facilities—A prospect for a brighter future for research with neutrons,"Neutron News, vol. 31, no. 2–4, pp. 13–18, Oct. 2020. doi:10.1080/10448632.2020.1819125

[6] LENS Ad hoc Working Group CANS, "Low energy accelerator-driven neutron sources," League of Advanced European Neutron Sources, Tech. Rep., Nov 2020.

[7] JCANS official website. https://www.jcans.net/rans.html

[8] ESS official website, https://www.europeanspallationsource.se/

[9] ILL official website, www.ill.eu.

[10] T. J. Roberts, "G4beamline Code Development", in *Proc. IPAC'12*, New Orleans, LA, USA, May 2012, paper MOPPC084, pp. 334–336.

[11] E. Mendoza, D. Cano-Ott, T. Koi, and C. Guerrero, "New Standard Evaluated Neutron Cross Section Libraries for the GEANT4 Code and First Verification,"*IEEE Trans. Nucl. Sci.*, vol. 61, no. 4, pp. 2357–2364, Aug. 2014. doi:10.1109/tns.2014.2335538

[12] A. Latina *et al.*, "A Compact Inverse Compton Scattering Source Based on X-Band Technology and Cavity-Enhanced High Average Power Ultrafast Lasers", in *Proc. LINAC'22*, Liverpool, UK, Aug.-Sep. 2022, pp. 44–46.doi:10.18429/JACoW-LINAC2022-MOPOJO09

[13] G. Geschonke and A. Ghigo, "Ctf3 design report," Rep. CERN-PS-2002-008-RF, Feb. 2009.